



ORIGINAL ARTICLE

A novel study on synthesis of egg shell based activated carbon for degradation of methylene blue via photocatalysis



Awais Ahmad^{a,*}, D. Jini^b, M. Aravind^b, C. Parvathiraja^c, Rabia Ali^d,
Maryam Zaheer Kiyani^e, Asma Alothman^f

^a Department of Chemistry, The University of Lahore, Lahore 54590, Pakistan

^b Department of Physics, Nanjil Catholic College of Arts and Science, Kaliyakkavilai, Kanyakumari, Tamil Nadu, India

^c Department of Physics, Manonmaniam Sundaranar University, Abishekapatti, Tirunelveli 627012, Tamil Nadu, India

^d Department of Chemistry, Quaid-e-Azam University, Islamabad, 15320 Islamabad, Pakistan

^e Department of Chemistry, Abdul Wali Khan University Mardan, Pakistan

^f Department of Chemistry, College of Science, King Saud University, Riyadh 11451, Saudi Arabia

Received 23 July 2020; accepted 1 October 2020

Available online 15 October 2020

KEYWORDS

Activated carbon;
Photocatalytic activity;
Methylene blue;
Hexagonal

Abstract Egg shell-based activated carbon was successfully synthesized by the simple chemical activation process. Orthophosphoric acid and sodium hydroxide used as an activation agent. XRD pattern reveals the hexagonal structure of activated carbon. The functional group presents in activated carbon was identified using FT-IR spectroscopy. SEM images show irregular shapes of carbon. The photocatalytic performance of investigated activated carbon by illuminating methylene blue dye under UV–Visible irradiations. Photocatalytic activity of activated carbon results maximum degradation efficiency of 83%. Adsorption efficiency have been increased with respect of time for degradation of dye. Free radicals and superoxide's play a significant role is decolorization of methylene blue. Photocatalytic activity of activated carbon synthesized by Orthophosphoric acid results shows the high degradation efficiency when compared to NaOH.

© 2020 The Author(s). Published by Elsevier B.V. on behalf of King Saud University. This is an open access article under the CC BY license (<http://creativecommons.org/licenses/by/4.0/>).

1. Introduction

In recent years, nanotechnology is a tool which has increasingly become an important topics for researchers to develop new devices using the nanoparticles to design, characterization of nanosized materials such as metal/metal oxide and from preparation aspects. These nanosized materials could potentially exposure in many different fields, such as drug delivery systems, biomedical-medicine, catalysis, and imag-

* Corresponding author.

E-mail address: awaisahmed@gcu.edu.pk (A. Ahmad).

Peer review under responsibility of King Saud University.



Production and hosting by Elsevier

ing/sensing etc. Among them, nanomaterials are appealing materials for applications as catalysis, due to their tremendous surface areas coupled with superior optical/electronic properties compared to larger-sized bulk materials (Erdoğan, 2020). Significant contributors to water pollution are textile industries that affect the biological oxygen demand level of water and pose a severe threat to aquatic fauna and flora. There are plenty of dyes which are present in water as pollutants and are troublesome to treat (Singh et al., 2017). Activated carbon have proven to be a tremendous substance by adsorbing the dye through chemical or physical bond over the surface to degrade dye and result in dye removal. The quality of Adsorption over the surface is owed to various physico chemical activities, including Pore volume, surface area, pore diameter(DP) and pore size distribution. Slight alteration in these properties greatly enhance the adsorption power of the activated charcoal (Kalantary et al., 2016; Zhao et al., 2020). Biomass such as Onion leaves (Hernández-Barreto et al., 2020) Sugar cane leaves (Li et al., 2016) Tobacco stalk (Bolbol et al., 2019), Cabbage (Zhang et al., 2019), Date palm (Alagha et al., 2020), Rice husk (He et al., 2019) Sewage sludge (Alagha, 2020), Tamarind seed (Andas and Satar, 2018), Teak saw dust (Armynah et al., 2014); Mosambi peels (Singh et al., 2019), Pea shells (Geçgel et al., 2013); Rubber wood sawdust (Kumar et al., 2005), Jute fiber (Senthilkumaar et al., 2005) and Mango seed kernel (Vasanth and Kumaran, 2005) have been utilized for the preparation of activated carbon. The chemical activation method which involves chemical activators such as H_3PO_4 , KOH and $ZnCl_2$ and then gets impregnated with resulting char. Execution of chemical activation can be achieved in a single step, whereas activation and carbonization are done simultaneously. A uni-step chemical activation method can scale down operational time, cost and energy consumption (Khanday et al., 2017). Porous carbonaceous absorbent, AC has better absorption ability than other absorbents (Marrakchi et al., 2016). Photocatalysis is time taking processes, due to the generation of electrons and holes pair via light that can easily recombine (Marrakchi et al., 2016). Various treatment techniques and strategies have been reported previously to eradicate the dyes from dye-bearing effluents. Among them, adsorption is a favourable method for eliminating coloured contaminants. This process is also significant for being a non-destructive process because it just involves the relocation of pollutants from one phase to another, rather than being eliminated. Therefore, the adsorbent regeneration is required prior to its reuse (Khanday et al., 2017).

In this present study, activated carbon was successfully synthesized by the chemical activation process with various activation agents. As the present investigation results, the comparison of Orthophosphoric acid and NaOH activation agent. Structural, morphological and optical properties of synthesized activated carbon were characterized using XRD, SEM and FT-IR spectroscopy. Methylene blue removal of activated carbon was experimentally visualized using a UV-Visible irradiation technique.

2. Materials and method

Egg shell was collected from the local market. Orthophosphoric acid and NaOH were purchased from Madras scientific

chemicals, Tirunelveli, India. Methylene blue was obtained from Merck.

2.1. Preparation of activated carbon

Egg shells were washed and dried at sunlight for a day. Crush the powder and grounded it into a very fine powder. The powdered egg shell was well mixed with a 4:1 ratio of an activating agent (NaOH and H_3PO_4) and egg shell. Stirrer the solution for an hour. Place the solution 24 h for the activation process. Filter the solution and dried for 550 °C for 3 h. Thus activated carbon is obtained. Obtained carbon was stored for further characterization.

2.2. Characterization of activated carbon (AC)

The structural and phase of investigated AC was investigated using XRD. Crystallographic patterns were recorded using PAN analytical XPERT PRO Diffractometer. FT-IR spectra were recorded using a Perkin Elmer spectrometer with KBr pellets. FT-IR spectra were recorded from 4000 to 600 cm^{-1} . Nano Metrix visualized the particle size of investigated activated carbon. The surface morphology of activated carbon was visualized using Joel JSM 6390 Scanning Electron microscope.

2.3. Photocatalytic activity

The dye degradation efficiency of activated carbon was recorded using UV-Visible irradiation. 50 ml/L of methylene blue is mixed with 0.50 g of active material. The mixture of activated carbon and methylene blue were well mixed using stirrer and centrifuged. Degradation of methylene blue removal was experimentally carried out using UV-Visible irradiations. The dye degradation efficiency of activated carbon was calculated using

$$\eta = \frac{(C_0 - C_t)}{C_t} \times 100$$

η - removal efficiency

C_0 . Initial concentration (mg/L) of methylene blue

C_t . Concentration of methylene blue at equilibrium (mg/L) (Zhang et al., 2019).

3. Results and discussion

3.1. XRD analysis

Crystal structure, micro strain, density dislocation and average crystalline size were calculated from the XRD spectrum. XRD pattern of activated carbon was shown in Fig. 1. X-ray diffraction peaks observed at 29.5°, 36.1°, 39.5°, 43.4°, 47.7°, 48.6°, and 57.7° corresponds to Bragg's reflection planes of (201), (105), (107), (207), (206), (304), and (314) respectively. Obtained diffraction peaks show the hexagonal crystal structure of carbon and well-matched with JCPDS: 721,616 (Amarasinghe and Wanniarachdhi, 2019). In addition to that peak at 23.1° corresponds to (012) reflection plane corre-

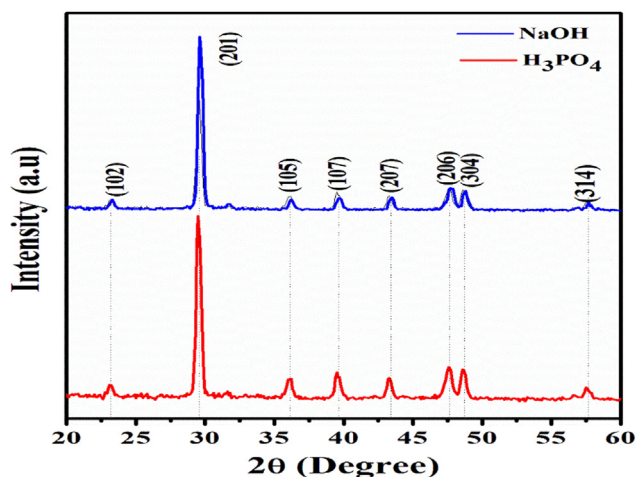


Fig. 1 XRD of Egg shell based activated carbon (XRD: X-ray diffraction).

sponds to the rhombohedral structure of CaCO_3 . From XRD pattern shows a mixed crystal phase with a hexagonal structure of carbon. Variations in average crystalline, change in peak intensity peak shift due to the influence of activating agent and egg shell components. For H_3PO_4 activated egg shell results in high crystalline peaks when compared to NaOH. The addition of NaOH activation agent results indicates the removal of silica and ash content. There is a slight variation in the XRD pattern of activated carbon due to the activation agent. Phosphoric acid increases the porous structure of carbon.

3.2. Fourier transform infrared Spectroscopy.

Functional group and chemical components present in egg shell based activated carbon were recorded using FT-IR spectroscopy. FT-IR spectra of AC is depicted in Fig. 2. The

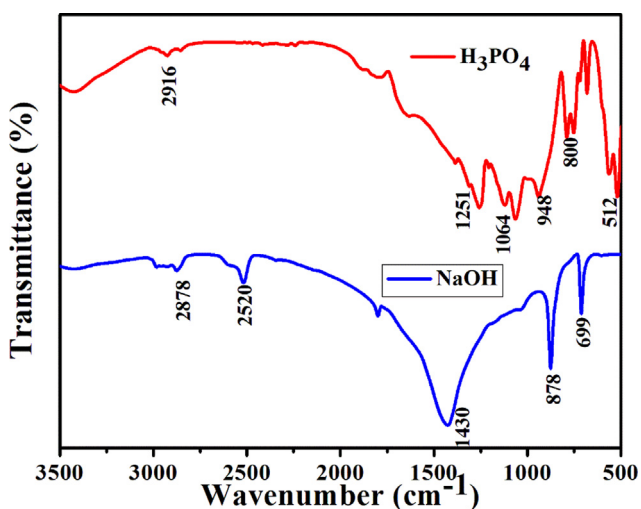


Fig. 2 FT-IR spectra of Egg shell based activated carbon (Red) H_3PO_4 (b) NaOH. (For interpretation of the references to colour in this figure legend, the reader is referred to the web version of this article.)

hydroxyl group presents at 3369 and 3359 cm^{-1} . The observed peak at 2916 and 2878 cm^{-1} corresponds to C–H interaction with the surface of the carbon. A climax at 1430 cm^{-1} attributed to the carbonate group vibration (Balasubramanian et al., 2019). The band observed at 1064 cm^{-1} corresponds to the vibration of the phosphate group. 948 corresponds to the vibration of calcium carbonate. The band observed at 878 and 800 cm^{-1} due to the vibration of carbonate. The peak observed at 699 cm^{-1} due to C–H vibration. A spike at 512 cm^{-1} represents the vibration of PO_4^{3-} (Tangboriboon et al., 2012). Change in peak intensity is due to Protoporphyrin IX pigment present in the egg shell. When phosphoric acid interacted with phenolic and carbonyl groups of carbon results P-Carbon (C-O-P). Formation of C–O–P bond results development of microspores on the surface of carbon (Shalma et al., 2008). The presence of nitrogen, oxygen, and hydrogen quickly bond with other metals on the surface. This result in decreasing activation energy for methylene blue degradation and more surface area to the activated sites on the AC (Luo, 2009).

3.3. Scanning electron microscope

The structural morphology of AC was visualized by implementing SEM technique. SEM images of activated carbon were shown in Fig. 3(a,b). The morphological view of activated carbon from the egg shell reveals irregular shape. Investigated activated carbon result ununiformed structure of carbon. The acid acts as a dehydration agent that inhibits tar formation. The calcination process enhances the surface area. Thermal effect or temperature is one of the most influencing factors for activated carbons. This process on the surface area forms the active sites. The active sites are known to be the material absorption process (Pezoti et al., 2016), which results in micropores present in activated carbon. Activated carbon prepared by NaOH the activation agent results from the smooth surface of carbon with less amount of microspores (Islam et al., 2015).

3.4. Particle size analyzer

The Average particle size value of investigated activated carbon shows 89 nm for NaOH activation and 88 nm for Orthophosphoric acid activation. DLS spectra of activated carbon were shown in Fig. 4. Investigated activated carbon results poly dispersive index of 0.765 and 0.57 respectively.

3.5. Photocatalytic activity

Photodegradation of methylene blue results in the absorption efficiency of activated carbon. Photocatalytic activity of activated carbon was experimentally studied using UV–Visible irradiation technique. Activated carbon used as an active source to degrade dye molecules. Photodegradation of activated carbon was recorded at every 30 min interval of time. Fig. 5.a and b. shows, photodegradation of methylene blue (see Fig. 6).

The UV–Visible absorption band of MB monomer in water molecules corresponds to 665 nm region which shows $n-\pi^*$ transition of MB (Ilomuanya and Igwilo, 2017). Excitation of electrons from the CB to VB generates a hole behind. Which causes photo to generate electron and spots on the surfaces of

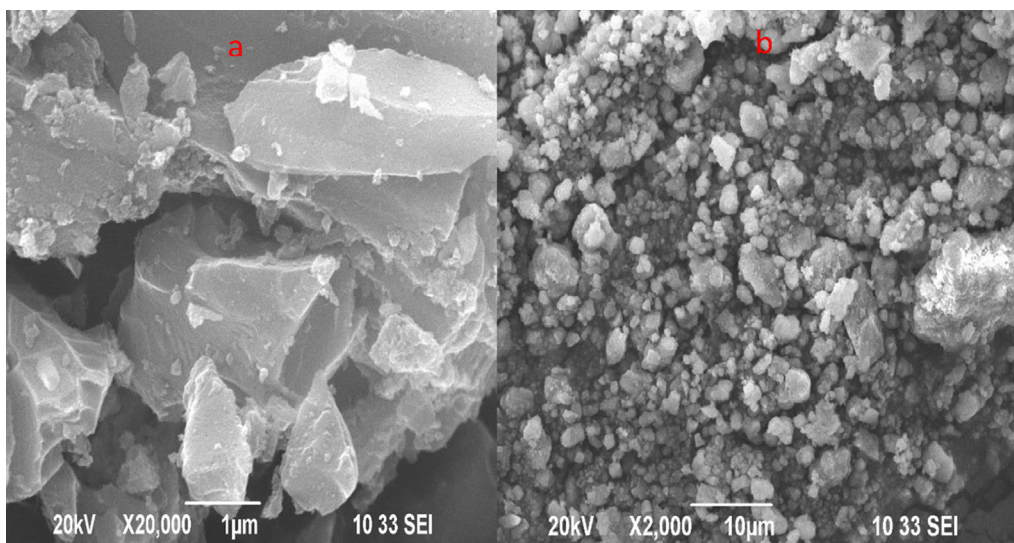


Fig. 3 FESEM images Egg shell based activated carbon (a), NaOH (b), H₃PO₄.

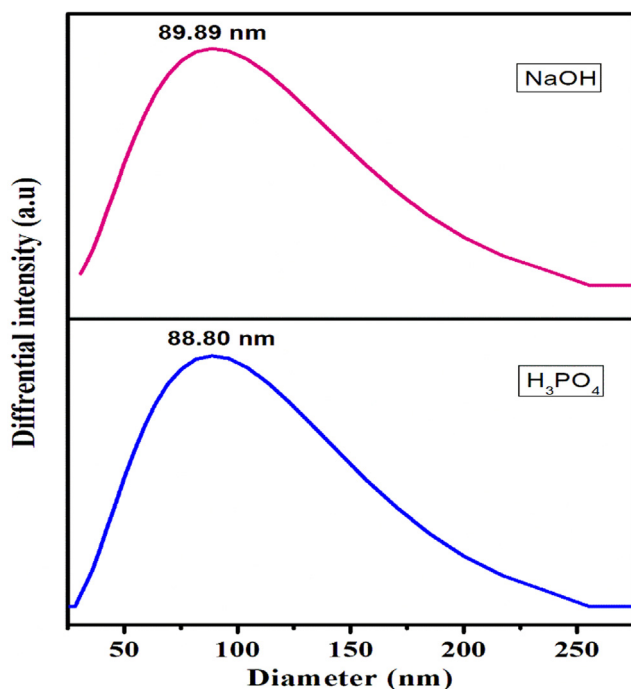
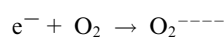
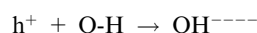
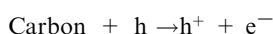


Fig. 4 DLS spectra of Egg shell based activated carbon.

the carbon OH group present in activated carbon interact with holes to form OH^\ominus free radical. Oxygen molecules interact with the carbon surface to form superoxide's ($\text{O}_2^{\cdot-}$). Organic pollutant (MB) can neutralize to H_2O and CO_2 and mineral acids present in activated carbon are responsible for dye removal (Jayakumar et al., 2017). Decolourization of methylene blue is due to the destruction of Azo bonds ($-\text{N}=\text{N}-$). During the degradation process, dye molecules were converted to leuco Methylene blue, which results in change the colour formation.



Activated carbon results show the maximum degradation efficiency of about 74% and 83% for NaOH activation and H₃PO₄ activated carbon. % R of methylene blue dye. % R at 0, 30, 60, 90, 120 and 150 min were 29.90, 45.17, 49.59, 76.09, and 83.96, respectively for H₃PO₄ and 32, 43, 56, 66, 68, 74 %R for NaOH (Ahmad et al., 2020). The absorption spectra reveal the degradation of MB from aqueous medium increases as the reaction time increases (Bagheri et al., 2015). The surface of AC is enriched mainly carboxyl, carbonyl, lactone, phenolic hydroxyl groups, and many oxygen-containing functional groups together, which determine its adsorption performance. There are three main modes of action which increase the photodegradation of MB, the first is to give electrons-to be affected by electrons, the second is electrostatic action, and the third is coordination reaction (Muzarpar et al., 2020). The photocatalytic activity results tell the fact of increases in methylene blue removal from 0 to 30 min. The degradation rate slows after 30 to 120 min for both samples. MB decomposes to leuco methylene blue after 120 min. The photocatalytic activity of AC prepared using (H₃PO₄) was higher when compared to NaOH. By adding phosphoric acid as an activation agent which gives the carbon results to C-O-P formation due to the carbon phosphorous formation to the surface. The results reassure the microspores distribution on the surface of AC. Active microspores present in the activated carbon results give high degradation efficiency when compared to NaOH. Degradation efficiency increases with high porosity, spectacular adsorption capacity, and enhanced active sites for the reacting species during chemical reaction (Hameed, 2020; Ramli et al., 2014; Huang et al., 2011; Hoseinzadeh Hesas et al., 2013; Foo and Hameed, 2012; Deng et al., 2010).

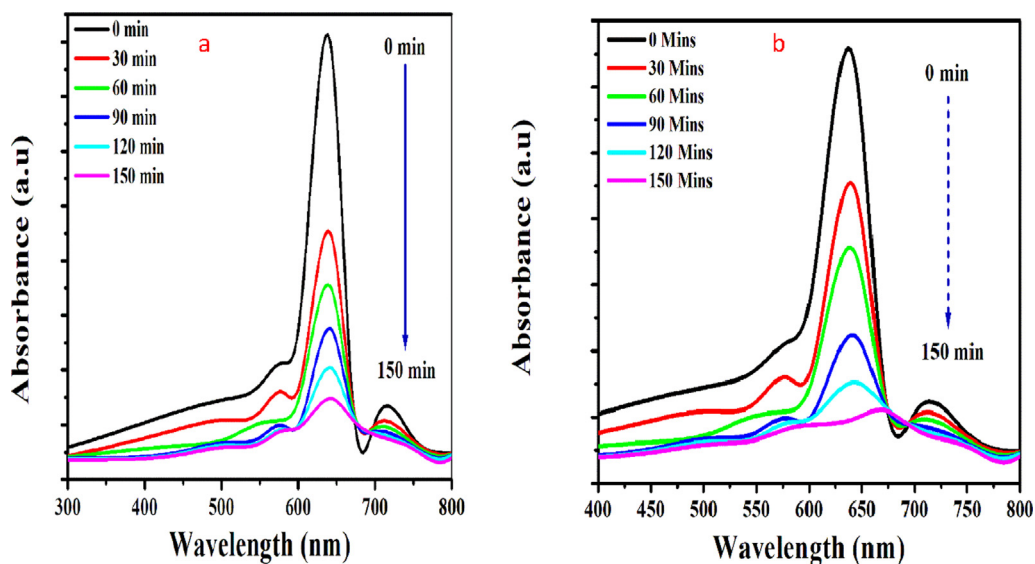


Fig. 5 shows Photocatalytic activity of Egg shell based activated carbon (a) With H₃PO₄ 84% (b) with NaOH 74%

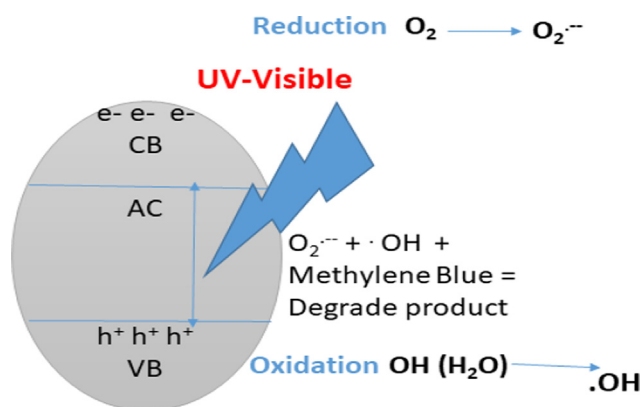


Fig. 6 Schematic representation about photocatalysis and its impact on degradation of organic pollutant i.e. Methylene Blue.

4. Conclusion

In this work, activated carbon was successfully synthesized by the chemical activation method. The rich amount of carbon having high absorbent due to the surface area and porous nature of the material. XRD pattern reveals a mixed phase of activated carbon with a hexagonal crystal structure of carbon. FT-IR identified the functional group present in activated carbon. Particle size increases for NaOH activation. SEM images reveal the irregular form of activated carbon with active microspheres. Photodegradation of activated carbon results maximum degradation efficiency of 83% at 120 min. Degradation efficiency rate increases from 0 to 30 min. From the photocatalytic activity of activated carbon results, the investigated activated carbon is highly applicable for wastewater treatment.

Declaration of Competing Interest

The authors declare that they have no known competing financial interests or personal relationships that could have appeared to influence the work reported in this paper.

Acknowledgements

This work was funded by the Researchers Supporting Project Number (RSP-2020/243) King Saud University, Riyadh, Saudi Arabia.

References

- Ahmad, Tokeer, Veenu, Nazim, Arasalan, Farooq, Umar, Khan, Huma, Jain, Sapan K., Ubaidullah, Mohd, Ahamed, Jahangeer, 2020. Biosynthesis, characterization and photocatalytic degradation of methylene blue removal using silver nanoparticles. *Mater. Today Proc.* <https://doi.org/10.1016/j.matpr.2020.04.707>.
- Alagha, O., Manzar, M.S., Zubair, M., Anil, I., Mu'azu, N.D., Qureshi, A., 2020. Comparative adsorptive removal of phosphate and nitrate from wastewater using Biochar-MgAl LDH nanocomposites: coexisting anions effect and mechanistic studies. *Nanomaterials* 2020 (10), 336. <https://doi.org/10.3390/nano10020336>.
- Alagha, Omar, Manzar, Mohammad Saood, Zubair, Mukarram, Anil, Ismail, Mu'azu, Nuhu Dalhat, Qureshi, Aleem, 2020. Magnetic Mg-Fe/LDH intercalated activated carbon composites for nitrate and phosphate removal from wastewater: insight into behavior and mechanisms. *Nanomaterials* 10, 1361. <https://doi.org/10.3390/nano10071361>.
- Amarasinghe, Achala, Wanniarachdhi, Dakshika, 2019. Eco-friendly photocatalyst derived from Eggshell waste for dye degradation. *J. Chem.*, 8184732
- Andas, Jeyashelly, Satar, Nur Asmidar Ab., 2018. Synthesis and characterization of tamarind seed activated carbon using different types of activating agents: a comparison study. *Mater. Today: Proc.* 5, 17611–17617.
- Armynah, B., Tahir, D., Jaya, N., 2014. Annealing effect on the particle size and chemical composition of activated carbon obtained from vacuum furnace of teak sawdust. *AIP Conf. Proc.* 1617, 19. <https://doi.org/10.1063/1.4897094>.
- Bagheri, Samira, Julkapli, Nurhidayatullaili Muhd, Hamid, Sharifah Bee Abd, 2015. Functionalised activated carbon derived from biomass for photocatalysis applications perspective. *Int. J. Photoenergy.* <https://doi.org/10.1155/2015/218743>.
- Balasubramanian, V., Daniel, T., Henry, J., Sivakumar, G., Mohanraj, K., 2019. Electrochemical performances of activated carbon prepared using eggshell waste, *SN. Appl. Sci.*

- Bolbol, H., Fekri, M., Hejazi-Mehrzi, M., 2019. Layered double hydroxide-loaded biochar as a sorbent for the removal of aquatic phosphorus: behavior and mechanism insights. *Arab. J. Geosci.* 12, 503. <https://doi.org/10.1007/s12517-019-4694-4>.
- Deng, H., Zhang, G., Xu, X., Tao, G., Dai, J., 2010. Optimization of preparation of activated carbon from cotton stalk by microwave assisted phosphoric acid-chemical activation. *J. Hazard. Mater.* 182, 2.
- Erdoğan, Meryem Kalkan, 2020. Preparation and stabilization of Ag nanoparticles with N-vinyl-2-pyrrolidone grafted-poly (vinyl alcohol) in an organic medium and investigation of their usability in the catalytic dye decolorization. *Colloid Interface Sci. Commun.* 34. <https://doi.org/10.1016/j.colcom.2019.100222>.
- Foo, K.Y., Hameed, B.H., 2012. Porous structure and adsorptive properties of pineapple peel based activated carbons prepared via microwave assisted KOH and K₂CO₃ activation. *Microporous Mesoporous Mater.* 148, 191–195.
- Gegel, Ünal, Özcan, Gülce, Gürpınar, Gizem Çağla, 2013. Removal of methylene blue from aqueous solution by activated carbon prepared from Pea Shells (*Pisum sativum*). *J. Chem.* 2013, Article ID 614083, 9p. <http://dx.doi.org/10.1155/2013/614083>.
- Hameed, Ahmed M., 2020. Synthesis of Si/Cu amorphous adsorbent for efficient removal of methylene blue dye from aqueous media. *J. Inorg. Organomet. Polym. Mater.* <https://doi.org/10.1007/s10904-019-01436-1>.
- He, H., Zhang, N., Chen, N., Lei, Z., Shimizu, K., Zhang, Z., 2019. Efficient phosphate removal from wastewater by MgAl-LDHs modified hydrochar derived from tobacco stalk. *Bioresour. Technol. Rep.* 8, <https://doi.org/10.1016/j.biteb.2019.100348> 100348.
- Hernández-Barreto, Diego Felipe, Rodríguez-Estupiñán, Jenny Paola, Moreno-Piraján, Juan Carlos, 2020. Adsorption and photocatalytic study of phenol using composites of activated carbon prepared from onion leaves (*Allium fistulosum*) and metallic oxides (ZnO and TiO₂). *Catalysts* 10, 574. <https://doi.org/10.3390/catal10050574>.
- Hoseinzadeh Hesas, R., Wan Daud, W.M.A., Sahu, J.N., Arami-Niya, A., 2013. The effects of a microwave heating method on the production of activated carbon from agricultural waste: a review. *J. Anal. Appl. Pyrolysis* 100, 1–11.
- Huang, L., Sun, Y., Wang, W., Yue, Q., Yang, T., 2011. Comparative study on characterization of activated carbons prepared by microwave and conventional heating methods and application in removal of oxytetracycline (OTC). *Chem. Eng. J.* 171, 1446–1453.
- Iloмуanya, Margaret O., Igwilo, Cecilia I., omuanya and Igwilo. Effect of pore size and morphology of activated charcoal prepared from midribs of *Elaeis Guineensis* on adsorption of poisons using metronidazole and *Escherichia coli* O157:H7 as a case study. *J. Microsc. Ultrastruct.* 4 (1), 32–38.
- Islam, M.A., Benhouria, A., Asif, M., Hameed, B.H., 2015. Methylene blue adsorption on factory-rejected tea activated carbon prepared by conjunction of hydrothermal carbonization and sodium hydroxide activation processes. *J. Taiwan Inst. Chem. Eng.* 52, 57–64.
- Jayakumar, G., AlbertIrudayaraj, A., DhyalRaj, A., 2017. Photocatalytic degradation of methylene blue by nickel oxide nanoparticles. *Mater. Today Proc.* 4, 11690–11695.
- Kalantary, R.R., Azari, A., Esrafil, A., Yaghmaeian, K., Moradi, M., Sharafi, K., 2016. The survey of Malathion removal using magnetic graphene oxide nanocomposite as a novel adsorbent: thermodynamics, isotherms, and kinetic study. *Desalin. Water Treat.* 57 (58), 28460–28473.
- Khanday, W.A., Asif, M., Hameed, B.H., 2017. Cross-linked beads of activated oil palm ash zeolite/chitosan composite as a bio-adsorbent for the removal of methylene blue and acid blue 29 dyes. *Int. J. Biol. Macromol.* 95, 895–902.
- Khanday, W., Marrakchi, F., Asif, M., Hameed, B.H., 2017. Mesoporous zeolite-activated carbon composite from oil palm ash as an effective adsorbent for methylene blue. *J. Taiwan Inst. Chem. Eng.* 70, 32–41.
- Kumar, B.G.P., Miranda, L.R., Velan, M., 2005. Adsorption of bismark brown dye on activated carbons prepared from rubberwood sawdust (*Hevea brasiliensis*) using different activation methods. *J. Hazard. Mater.* 126 (1–3), 63–70.
- Li, R., Wang, J.J., Zhou, B., Awasthi, M.K., Ali, A., Zhang, Z., Gaston, L.A., Lahori, A.H., Mahar, A., 2016. Enhancing phosphate adsorption by Mg/Al layered double hydroxide functionalized biochar with different Mg/Al ratios. *Sci. Total Environ.* 559, 121–129. <https://doi.org/10.1016/j.scitotenv.2016.03>.
- Luo, Yiping, Li, Dong, Liu, Xiaofeng, 2009. The performance of phosphoric acid in the preparation of activated carbon-containing phosphorous species from rice husk residue. *J. Mater. Life Sci.* 54, 5008–5021.
- Marrakchi, F., Ahmed, M.J., Khanday, W.A., Asif, M., Hameed, B. H., 2016. Mesoporous-activated carbon prepared from chitosan flakes via single-step sodium hydroxide activation for the adsorption of methylene blue. *Int. J. Biol. Macromol.* 98, 233–239.
- Marrakchi, F., Khanday, W.A., Asif, M., Hameed, B.H., 2016. Cross-linked chitosan/sepiolite composite for the adsorption of methylene blue and reactive orange 16. *Int. J. Biol. Macromol.* 93, 1231–1239.
- Muzarpar, M.S., Leman, A.M., Rahman, K.A., Shayfull, Z., Irfan, A. R., 2020. Exploration sustainable base material for activated carbon production using agriculture waste as raw materials: a review. *IOP Conf. Series: Mater. Sci. Eng.* 864. <https://doi.org/10.1088/1757-899X/864/1/012022>.
- Pezoti, O., Cazetta, A.L., Bedin, K.C., Souza, L.S., Martins, A.C., Silva, T.L., Santos Júnior, O.O., Visentainer, J.V., Almeida, V.C., 2016. NaOH-activated carbon of high surface area produced from guava seeds as a high-efficiency adsorbent for amoxicillin removal: Kinetic, isotherm and thermodynamic studies. *Chem. Eng. J.* 288, 778–788.
- Ramli, Zatil Amali Che, Asim, Nilofar, Isahak, Wan N.R.W., Emdadi, Zeynab, Ahmad-Ludin, Norasikin, Ambar Yarmo, M., Sopian, K., 2014. Photocatalytic degradation of methylene blue under UV light irradiations on prepared carbonaceous TiO₂. *Sci. World J.* <https://doi.org/10.1155/2014/415136>.
- Senthilkumaar, S., Varadarajan, P.R., Porkodi, K., Subbhuraam, C. V., 2005. Adsorption of methylene blue onto jute fiber carbon: kinetics and equilibrium studies. *J. Colloid Interface Sci.* 284 (1), 78–82.
- Shalma, K., Boradajenko, N., Plata, A., 2008. Fourier transform infrared spectra of technologically modified calcium phosphate. *RTU Res. Inf. Syst.*, 68–71
- Singh, Sonika, Sidhu, Gurjiwan Kaur, Singh, Harminder, 2017. Removal of methylene blue dye using activated carbon prepared from biowaste precursor. *Indian Chem. Eng.* <https://doi.org/10.1080/00194506.2017.1408431>.
- Singh, Sonika, Sidhu, Gurjiwan Kaur, Singh, Harminder, 2019. Removal of methylene blue dye using activated carbon prepared from biowaste precursor. *Indian Chem. Eng.* ISSN: 0019-4506 (Print) 0975-007X.
- Tangboriboon, N., Kunanuruksapong, R., Irvan, A.S., 2012. Preparation of calcium oxide from egg shell via calcination. *Mater. Sci.*, 31–322
- Vasanth, K., Kumaran, A., 2005. Removal of methylene blue by mango seed kernel powder. *Biochem. Eng. J.* 27 (1), 83–93.
- Zhang, Z., Yan, L., Yu, H., Yan, T., Li, X., 2019. Adsorption of phosphate from aqueous solution by vegetable biochar/layered double oxides: fast removal and mechanistic studies. *Bioresour. Technol.* 284, 65–71. <https://doi.org/10.1016/j.biortech.2019.03.113>.
- Zhao, Y., Min, X., Ding, Z., Chen, S., Ai, C., Liu, Z., Huang, Z., 2020. Metal-based nanocatalysts via a universal design on cellular structure. *Adv. Sci.* 7 (3), 1902051.